



Thermoeconomic Analysis of Solar Chimney and Wind Turbine Application to Help Generate Electricity in a Trigeneration Cycle

B. Khorram, I. Mirzaee*, S. Jafarmadar

Department of Mechanical Engineering, Faculty of Engineering, Urmia University, Urmia, Iran

PAPER INFO

Paper history:

Received 11 February 2022

Accepted in revised form 17 April 2022

Keywords:

Multigeneration
Parabolic dish collector
Solar chimney
Thermoeconomic analysis
Wind turbine

ABSTRACT

The main purpose of this study is to evaluate the thermodynamic and economic performance of using a solar chimney and wind turbine to help generate electricity in a multigeneration system. The proposed system is designed to generate power, heating, cooling, hot water, and steam. Parametric studies were conducted to evaluate the effects of various parameters such as Brayton cycle turbine inlet pressure, organic Rankine cycle turbine inlet temperature, solar radiation, wind speed, and absorption refrigeration cycle evaporator temperature on the system efficiency. The effects of these parameters on the energy, exergy, and economic efficiencies of the whole system were investigated. The results showed that the highest energy efficiency and total exergy of the multigeneration system were 22.12% and 11.4%, respectively. Also, the total power generation capacity of the studied system was calculated to be 2103 kW. The results also depicted that the highest rate of exergy destruction for the main components of the system is found in the parabolic dish solar collector. Increasing the turbine inlet pressure, the average wind velocity of the wind turbine and, evaporator temperature increasing of absorption refrigeration cycle has a positive effect on the efficiency of the proposed system.

doi: 10.5829/ijee.2022.13.03.02

NOMENCLATURE

A	Heat transfer area (m ²)	D	Destruction
\dot{C}	Cost rate (\$/y)	DWH	Domestic water heater
c	Cost per unit exergy (\$/GJ)	eva	Evaporator
ex	Specific exergy (kJ/kg)	exv	Expansion valve
$\dot{E}x$	Exergy rate (kW)	g	Generator
h	Specific enthalpy (kJ/kg)	GT	Gas turbine
\dot{m}	Mass flow rate (kg/s)	HX	Heat exchanger
P	Pressure (MPa)	net	Net
\dot{Q}	Heat transfer rate (kW)	$OFWH$	Open feedwater heater
T	Temperature (°C)	p	Pump
\dot{W}	Power (kW)	$PDSC$	Parabolic dish collector
z	The capital cost of components (\$)	SC	Solar chimney
\dot{Z}	Capital cost rate (\$/y)	t	Turbine
		wt	Wind turbine

Subscripts

0	Environmental state
1, 2, 3, ...	Cycle points

abs	Absorber
con	Condenser

Greek Symbols

ρ	Density (kg/m ³)
η	Efficiency (%)

*Corresponding Author Email: Lmirzaee@urmia.ac.ir (I. Mirzaee)

Please cite this article as: B. Khorram, I. Mirzaee, S. Jafarmadar, 2022. Thermoeconomic Analysis of Solar Chimney and Wind Turbine Application to Help Generate Electricity in a Trigeneration Cycle, Iranian (Iranica) Journal of Energy and Environment, 13(2), pp.220-230. Doi: 10.5829/ijee.2022.13.03.02

INTRODUCTION

The use of fossil fuels to meet electrical needs has created many problems, including CO₂ emissions, ozone depletion, climate change, rising electricity prices, and acid rain [1, 2]. Solar energy is the best alternative to overcome such challenges because it is clean, cheap, and widely available worldwide. In solar thermal systems, the incoming radiation is absorbed by the solar collectors and then converted into energy by converting energy into the operating fluid into useful thermal energy[3]. Solar energy concentrating technologies are receiving more attention in high and medium temperature ranges due to their higher thermal efficiency. Plate systems can be integrated with the organic Rankine cycle[4], Stirling engines [5], micro-gas turbines, and the steam Rankine cycle[6].

Various thermodynamic cycles (Brayton cycle, steam cycle, etc.) are used to convert solar thermal energy into useful energy such as electricity. The cost of generating electricity can be significantly reduced by reducing heat dissipation, and combined gas cycles have received a great deal of attention due to their higher thermal efficiency than gas or steam cycles. In combined power cycles, gas cycles, which are upstream, operate at significantly higher temperatures. Hence, the gas cycles act as the primary power cycles, and a large amount of the heat released by them is used to guide the steam cycles as well as for reheating [7].

Solar chimney technology does not require tracking devices or specialized construction materials. In addition, the solar chimney is not affected by high temperatures and has a low operating cost. Although the studies about the different uses of solar chimneys have increased in recent years; there is a need to investigate the different aspects of applying solar chimneys and integrating them with other cycles. Therefore, in the present study, the feasibility of using solar chimneys and wind energy as leading technologies is examined.

Haaf et al. [8] were among the first researchers to test a prototype solar chimney plant in Manzanares, Spain in 1983. They reported that the output power of the solar chimney power plant was 50 kW in 1000 W/m² solar radiation. Zandian and Ashjaei [9] proposed a concept in which the cooling tower of Shahid Rajaei power plant was replaced by a solar chimney. The results showed that the output power of the solar chimney power plant was 360 kW to 3 MW at different diameters of the chimney.

The use of hybrid cycles that use solar energy, gas turbines, or wind turbines as an energy source has been studied by many researchers. A new integrated system for residential applications including wind turbines and a solar plate collector for renewable energy extraction, an Organic Rankine cycle for power generation, and an absorption chiller for cold generation was introduced by

Esfandi et al. [10]. The results showed that the combined methane production of this system varies from 42 to 140 cubic meters per month, due to carbon dioxide consumption from 44 to 144 cubic meters per month for duration of one year. In addition, the energy efficiency and exergy of this hybrid system vary from 24.7% and 23% to 9.1% and 8%, respectively. The simple payback time for the studied integrated system was 15.6 years while the payback time of the hybrid cycle was 21.4 years. Méndez and Bicer [11] studied the feasibility of using an integrated system to generate electricity and freshwater, using solar chimneys and wind energy as their main technologies. Preliminary analysis was performed to evaluate power generation and heat absorption by the solar chimney storage system. In addition, waterfall thermal and membrane desalination technologies were incorporated to produce freshwater, using the heat storage heat source of a solar chimney. A wind farm was added to generate more electricity while meeting the demand of several systems. As a result, the integrated system offers overall energy efficiency of 52.53% when draining the water tank and 52.51% when storing water. Khan et al. [12] introduced a new multigeneration system that uses solar power to generate electricity, cooling, hydrogen, and freshwater. The system includes a parabolic plate collector with composite nanofluids, a Brayton carbon dioxide compression cycle, a proton exchange membrane electrolyzer, a desalination unit, and a dual lithium bromide absorption cycle. The results showed that the total energy efficiency and exergy of the proposed system are 31.59% and 30.02%, respectively. While the production of fresh water and cooling loads are 1.546 kg/s and 1.196 kW, respectively. The results of the economic analysis showed that the cost of electricity and the total rate of exergy destruction is 0.887 \$/kWh and 530 \$/h, respectively, with a repayment period of 9.5 years.

A review of previous studies has shown that the study of a combined power plant with a parabolic dish solar collector has rarely been studied. Researchers have mostly used heliostat solar towers and linear parabolic collectors for use in multigeneration systems, but the use of plate solar collectors for such purposes has rarely been studied. Also, no study has been done on the simultaneous use of solar chimneys and wind turbines to help generate electricity for such a system. Therefore, the present study aims to generate electricity using a combined cycle power plant that includes. Also, two solar chimney systems and wind turbines have been used to increase power generation in the proposed cycle. In addition, in the proposed cycle, instead of fossil fuels, renewable energy is used, which reduces the amount of carbon dioxide and is towards sustainable development.

System description

In the proposed system, a multigeneration cycle is designed for electricity, steam, hot water, cooling for

sustainable development. The schematic diagram of the proposed system is shown in Figure 1. The system consists of five sub-cycles: The Brayton cycle, the Organic Rankine cycle, an absorption cooling system, a steam generating unit, and a domestic hot water production system. A solar chimney and wind turbine (with an electricity generator) have also been used to help generate more electricity in the system under study. Fluid R123 is used as an operating fluid in the Organic Rankine cycle due to its environmentally friendly properties. Lithium bromide-water is also used as the operating fluid in absorption refrigeration cycles.

First, the compressed air is heated using a parabolic dish solar collector and transferred to a turbine to generate electricity. The heat leaving the Brayton cycle enters the heat exchanger of the steam generating system to provide the heat needed to generate steam. The air stream then enters the second heat exchanger to generate the heat required for the Organic Rankine cycle. The output stream then passes through the absorption cycle system to provide heating and cooling. The output current of the generator is used to heat the incoming water at a temperature of 25 °C and then the gas flow is discharged into the atmosphere after the temperature decreases. Also, a solar chimney and wind turbine are used for power production.

Thermodynamic and economic analysis

Thermodynamic analysis of the proposed system is performed by the EES program [13]. The thermodynamic calculations of the general system and subsystems are determined in this section. Design parameters and assumptions for thermodynamic analysis are presented in Table 1.

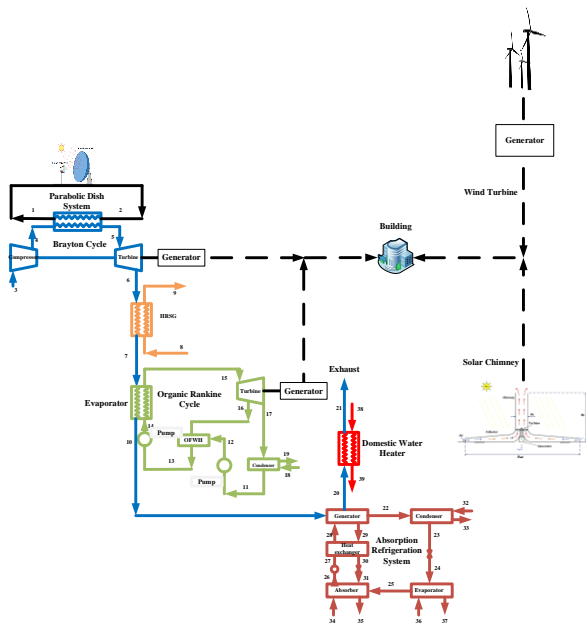


Figure 1. Schematic diagram of the proposed system

The following equations are used to calculate the properties of the Parabolic dish solar collector, Solar chimney, and wind turbine:

$$\eta_{en.,PDSC} = \frac{Q_u}{Q_{sun}} \tag{1}$$

Table 1. Input design conditions for the proposed system

Parameter	Value
Parabolic dish solar collector [6]	
Aperture area (m ²)	30.269
Receptor area (m ²)	0.0099
Inlet temperature (°C)	177
Solar radiation (W/m ²)	850
Mass flow rate (kg/s)	0.01
Optical efficiency (%)	85
Collector efficiency coefficient	0.9
Brayton cycle [14]	
Compressor isotropic efficiency (%)	85
Turbine isotropic efficiency (%)	85
Mass flow rate (kg/s)	10
Compressor outlet pressure (kPa)	1267
Steam generation system	
Mass flow rate (kg/s)	3.5
Production steam pressure (kPa)	2000
Organic Rankine cycle [15]	
Condenser temperature (°C)	40
Turbine inlet temperature (°C)	120
Open feedwater heater pressure (kPa)	494
Absorption refrigeration system [16]	
Mass flow rate (kg / s)	0.2
Evaporator temperature (°C)	5
Generator temperature (°C)	80
Condenser temperature (°C)	35
Absorber temperature (°C)	35
Solar chimney	
Collector diameter (m)	280
Chimney diameter (m)	14
Chimney height (m)	280
Wind turbine [17]	
Wind turbine diameter (m)	34
Average wind speed (m / s)	5.5
Turbine power factor	0.593

where Q_{sun} is defined as follows:

$$Q_{sun} = G_b A_{ap} \quad (2)$$

where G_b is the solar radiation falling on the solar concentrator and A_{ap} is the area of the aperture.

The useful energy Q_u available by the solar system is defined as follows:

$$Q_u = Q_r - Q_l \quad (3)$$

where Q_r is the solar energy radiation falling on the receiver and Q_l is the heat loss from the receiver and is obtained as follows:

$$Q_l = U_L A_r (T_r - T_0) \quad (4)$$

where U_L is the overall heat loss coefficient:

$$U_L = \left[\frac{A_r}{A_c (h_{c,ca} + h_{r,ca})} + \frac{1}{h_{r,cr}} \right]^{-1} \quad (5)$$

The useful heat gain of the concentrating solar system can be calculated by applying the famous Hottel-Whillier equation [13].

$$Q_u = F_r A_r \left[\left(S - \frac{A_r}{A_a} \right) U_l (T_{in} - T_a) \right] \quad (6)$$

where S is the absorbed radiation ($S = \eta_0 G_b$) and η_0 is the optical efficiency or thermal performance of the parabolic dish collector. Heat removal factor can be expressed as follows [18]:

$$F_R = \frac{\dot{m} C_p}{A_r U_L} \left[1 - \exp \left(\frac{-A_r U_L F_l}{\dot{m} C_p} \right) \right] \quad (7)$$

where F_l can be defined as follows:

$$F_l = \frac{U_0}{U_L} \quad (8)$$

$$U_0 = \frac{1}{U_l} + \frac{D_{r0}}{h_f D_{ri}} + \left[D_{r0} \ln \left(\frac{D_{r0}}{2.K} \right) \right]^{-1} \quad (9)$$

The total solar exergy content is estimated by using Patella's approach:

$$\dot{Ex}_{solar} = G_b A_a \left(1 - \frac{4T_0}{3T_{sun}} + \frac{1}{3} \left(\frac{T_0}{T_{sun}} \right)^4 \right) \quad (10)$$

The work output of the solar chimney turbine is calculated as:

$$\dot{W}_{sct} = \eta_{sct} \Delta P_{sct} \dot{v} \quad (11)$$

in which η_{sct} is the turbine efficiency, ΔP_{sct} is the pressure drop across the turbine and \dot{v} is the volume flow rate. The energy and exergy efficiencies of the solar chimney is presented as follows:

$$\eta_{en,sc} = \frac{\dot{W}_{sct}}{\frac{1}{4} \pi (D_{coll}^2 - D_{ch}^2) \dot{Q}_{rad}} \quad (12)$$

$$\eta_{ex,sc} = \frac{\dot{W}_{sct}}{\frac{1}{4} \pi (D_{coll}^2 - D_{ch}^2) \dot{Q}_{rad}} \quad (13)$$

In order to find the power output from the wind turbine the following equation is used:

$$P_{wt} = \frac{1}{2} \eta_{wt} \rho_{air} A_{wt} C_p V^3 \quad (14)$$

where ρ is the air density, V is the wind speed, A is the turbine's rotor area and C_p is the turbine's power coefficient.

The total exergy content of the wind turbine is:

$$\dot{Ex}_{wt} = \frac{1}{2} \rho_{air} A_{wt} V^3 \quad (15)$$

The equations used to estimate the energy efficiency and exergy of the system are as follows:

Mode 1: Multigeneration including parabolic plate solar collector, Brayton cycle, steam generation, Organic Rankine cycle, absorption refrigeration cycle, and domestic hot water

$$\eta_{en, state1} = \frac{\dot{W}_{net} + \dot{Q}_{HRSG} + \dot{Q}_{ARC,eva} + \dot{Q}_{DWH}}{\dot{Q}_{sun,PDSC}} \quad (16)$$

$$\eta_{ex, state1} = \frac{1}{\dot{Ex}_{solar}} \times \dot{W}_{net} + \dot{m}_{37} ex_{37} - \dot{m}_{36} ex_{36} + \dot{m}_{39} ex_{39} - \dot{m}_{38} ex_{38} + \dot{m}_9 ex_9 - \dot{m}_8 ex_8 \quad (17)$$

Mode 2: The first mode plus wind turbine

$$\eta_{en, state2} = \frac{\dot{W}_{net} + \dot{Q}_{HRSG} + \dot{Q}_{ARC,eva} + \dot{Q}_{DWH} + \dot{W}_{wt}}{\dot{Q}_{sun,PDSC} + \dot{W}_{wt}} \quad (18)$$

$$\eta_{ex, state2} = \frac{1}{\dot{Ex}_{solar} + \dot{Ex}_{wt}} \times \dot{W}_{net} + \dot{m}_{37} ex_{37} - \dot{m}_{36} ex_{36} + \dot{m}_{39} ex_{39} - \dot{m}_{38} ex_{38} + \dot{m}_9 ex_9 - \dot{m}_8 ex_8 + \dot{W}_{wt} \quad (19)$$

Mode 3: The second mode plus solar chimney

$$\eta_{ex, state 3} = \frac{\dot{W}_{net} + \dot{Q}_{HRSG} + \dot{Q}_{ARC,eva} + \dot{Q}_{DWH} + \dot{W}_{wt} + \dot{W}_{sc}}{\dot{Q}_{sum,PDSC} + \dot{W}_{wt} + \dot{Q}_{sum,sc}} \quad (20)$$

$$\eta_{ex, state 3} = \frac{1}{\dot{E}x_{solar} + \dot{E}x_{wt}} \times \dot{W}_{net} + \dot{m}_{37}ex_{37} - \dot{m}_{36}ex_{36} + \dot{m}_{39}ex_{39} - \dot{m}_{38}ex_{38} + \dot{m}_9ex_9 - \dot{m}_8ex_8 + \dot{W}_{wt} + \dot{W}_{sc} \quad (21)$$

Table 2 summarized cost balance, auxiliary equations, and investment cost equations.

RESULTS AND DISCUSSION

In this study, the EES program is used for all system thermodynamic calculations. The main thermodynamic and thermo-economic results are calculated at each point and presented in Table 3.

The rate of power generation in the sub-cycles of the system is shown in Figure 2. As it can be seen in Figure 2, it is clear that the highest power generation is in the Brayton cycle and the lowest power generation is in the organic Rankine cycle. The amount of power generated by Brayton cycle turbines, organic energy costs, solar chimneys, and wind turbines are 5486, 48.16, 115, and 197.5 kW, respectively. The reason the Brayton cycle produces more power is that it operates at very high temperatures.

The amount of exergy destruction of the main components of the overall system is shown in Figures 3a and 3b. As can be seen from the results, the greatest amount of exergy destruction is observed in the solar collector. The exergy destruction rate of the solar collector is 23957 kW. The Brayton and Organic Rankine cycles have the maximum amount of exergy destruction. Among the cycle components, the Brayton turbine and compressor and the Organic Rankine cycle evaporator have the highest exergy destruction rates. The cause of high destruction in the mentioned components is the large

Table 2. Cost balance, auxiliary, and investment equipment cost equations for each component of the proposed system [12, 19-21].

Components	Equipment cost	Cost equations	Auxiliary equations
PDSC	$Z_{PDSC} = 50.A_a$	$\dot{c}_{sum} + \dot{c}_1 + \dot{Z}_{PDSC} = \dot{c}_2$	$c_{sum} = 0$ $c_1 = c_2$
Brayton Compressor	$Z_{GT,c} = \left[\frac{71.1\dot{m}_3}{0.9 - \eta_{GT,c}} \right] \times \frac{P_4}{P_3} \times \ln \frac{P_4}{P_3}$	$\dot{c}_4 = \dot{Z}_{GT,c} + \dot{c}_{w,c} + \dot{c}_3$	$c_3 = 0$ $c_{w,GT,c} = c_{w,GT,t}$
Brayton Turbine	$Z_{GT,t} = \left[\frac{479.34\dot{m}_5}{0.9 - \eta_{GT,t}} \right] \times \frac{P_5}{P_6} \times (1 + \exp(0.036T_5 - 54.4))$	$\dot{c}_5 + \dot{Z}_{GT,t} = \dot{c}_{w,t} + \dot{c}_6$	$c_5 = c_6$
HRSG	$Z_{HRSG} = 130. \left(\frac{A_{HRSG}}{0.093} \right)^{0.78}$	$\dot{c}_6 + \dot{c}_8 + \dot{Z}_{HRSG} = \dot{c}_7 + \dot{c}_9$	$c_8 = 0$ $c_6 = c_7$
ORC Evaporator	$Z_{ORC,eva} = 309.14 (A_{ORC,eva})^{0.85}$	$\dot{c}_7 + \dot{c}_{14} + \dot{Z}_{ORC,eva} = \dot{c}_{10} + \dot{c}_{15}$	$c_7 = c_{10}$
ORC Pump 1	$Z_{ORC,p1} = 200 (\dot{W}_{ORC,p1})^{0.65}$	$\dot{c}_{12} = \dot{Z}_{ORC,p1} + \dot{c}_{w,p1} + \dot{c}_{11}$	$c_{w,p1} = c_{w,t}$
ORC Pump 2	$Z_{ORC,p2} = 200 (\dot{W}_{ORC,p2})^{0.65}$	$\dot{c}_{14} = \dot{Z}_{ORC,p2} + \dot{c}_{w,p2} + \dot{c}_{13}$	$c_{w,p2} = c_{w,t}$
ORC Turbine	$Z_{ORC,t} = 4750 (\dot{W}_{ORC,t})^{0.75}$	$\dot{c}_{15} + \dot{Z}_{ORC,t} = \dot{c}_{w,t} + \dot{c}_{16} + \dot{c}_{17}$	$c_{15} = c_{16}$ $c_{15} = c_{17}$

ORC Condenser	$Z_{ORC,com} = 516.62 \left(A_{ORC,com} \right)^{0.6}$	$\dot{c}_{17} + \dot{c}_{18} + \dot{Z}_{ORC,com} =$	$c_{18} = 0$
		$\dot{c}_{11} + \dot{c}_{19}$	$c_{17} = c_{11}$
ORC OFWH	$Z_{ORC,OFWH} = 0$	$\dot{c}_{12} + \dot{c}_{16} + \dot{Z}_{ORC,OFWH} =$	-
		\dot{c}_{13}	
ARC Generator	$Z_{ARC,g} = 17500 \cdot \left(\frac{A_{ARC,g}}{100} \right)^{0.6}$	$\dot{c}_{10} + \dot{c}_{28} + \dot{Z}_{ARC,g} =$	$c_{10} = c_{20}$
		$\dot{c}_{20} + \dot{c}_{22} + \dot{c}_{29}$	
ARC Condenser	$Z_{ARC,com} = 8000 \cdot \left(\frac{A_{ARC,com}}{100} \right)^{0.6}$	$\dot{c}_{22} + \dot{c}_{32} + \dot{Z}_{ARC,com} =$	$c_{22} = c_{23}$
		$\dot{c}_{23} + \dot{c}_{33}$	$c_{32} = 0$
ARC Evaporator	$Z_{ARC,eva} = 16000 \cdot \left(\frac{A_{ARC,eva}}{100} \right)^{0.6}$	$\dot{c}_{24} + \dot{c}_{26} + \dot{Z}_{ARC,eva} =$	$c_{24} = c_{25}$
		$\dot{c}_{25} + \dot{c}_{37}$	$c_{36} = 0$
ARC Absorber	$Z_{ARC,abs} = 16000 \cdot \left(\frac{A_{ARC,abs}}{100} \right)^{0.6}$	$\dot{c}_{25} + \dot{c}_{31} + \dot{c}_{34} + \dot{Z}_{ARC,abs}$	$c_{34} = 0$
		$= \dot{c}_{26} + \dot{c}_{35}$	
ARC Pump	$Z_{ARC,p} = 2100 \cdot \left(\frac{\dot{W}_{ARC,p}}{10} \right)^{0.26} \times$ $\left(\frac{1 - \eta_{ARC,p}}{\eta_{ARC,p}} \right)^{0.5}$	$\dot{c}_{27} = \dot{Z}_{ARC,p} + \dot{c}_{w,p}$	$c_{w,p} = c_{w,t}$
		$+ \dot{c}_{26}$	
ARC Expansion valve 1	$Z_{ARC,exv1} = 0$	$\dot{c}_{23} + \dot{Z}_{ARC,exv1} = \dot{c}_{24}$	-
ARC Expansion valve 2	$Z_{ARC,exv2} = 0$	$\dot{c}_{30} + \dot{Z}_{ARC,exv2} = \dot{c}_{31}$	-
ARC Heat exchanger	$Z_{ARC,HX} = 12000 \cdot \left(\frac{A_{ARC,HX}}{100} \right)^{0.6}$	$\dot{c}_{27} + \dot{c}_{29} + \dot{Z}_{ARC,HX}$	$c_{29} = c_{30}$
		$= \dot{c}_{28} + \dot{c}_{30}$	
DWH	$Z_{DWH} = 0.3 \times \dot{m}_{20}$	$\dot{c}_{20} + \dot{c}_{38} + \dot{Z}_{DWH}$	$c_{20} = c_{21}$
		$= \dot{c}_{21} + \dot{c}_{39}$	$c_{38} = 0$
Wind turbine	$Z_{WT} = 5000 \times \dot{W}_{WT}$	-	-
Solar chimney collector	$Z_{SC,coll} = 8.004 \times A_{SC,coll}$	-	-
Solar chimney tower	$Z_{SC,tow} = 80.04 \times H_{SC,tow} +$ $400.2 \times D_{SC,tow}^2$	-	-
Solar chimney turbine	$Z_{SC,t} = 400.2 \times \dot{W}_{SC,t}$	-	-

temperature difference between their input and output streams, which causes a large amount of exergy to be lost. Therefore, to have an effective system, it is necessary to be careful in selecting and designing these three components.

Figure 4 shows the energy and exergy efficiency of the studied systems. The three systems under consideration are: the first system includes parabolic plate solar collector cycles, Brayton cycle, a steam generation unit, Organic Rankine cycle, absorption refrigeration cycle,

and domestic water heater, the second system included the first system plus wind turbine and the third system contains the second system plus a solar chimney.

Examining the obtained diagrams, it is concluded that

adding a wind turbine to the introduced system increases the energy and exergy efficiency of the system, but adding a solar chimney reduces the efficiency of the system. Adding a solar chimney due to its large area

Table 3. The main thermodynamic and economic results of the studied system

State	P (kPa)	T (K)	$\dot{E}x(kW)$	\dot{C} (\$/y)
1	101	450	0.4345	5.775
2	101	1267.31	8.248	109.6
3	101	298.15	3.47	0
4	1267	660.31	6.932	158.5
5	1267	1202.53	11.03	196.4
6	101	717.46	5.115	91.05
7	101	449.66	3.764	67
8	2000	298.15	6.663	0
9	2000	485.53	642.6	24591
10	101	385.19	3577	63674
11	154.7	313.15	1.452	34.17
12	494	313.31	2.188	65.05
13	494	353.49	21.62	646.1
14	1201	353.94	23.79	845.9
15	1201	393.15	175.5	4131
16	494	364.62	25.94	610.3
17	154.7	336.12	30.31	713.1
18	101	298.15	0	0
19	101	308.15	9.18	920.2
20	101	377.24	3560	63361
21	101	332.24	3487	62077
22	5.629	353.15	17.47	1788
23	5.629	308.15	0.118	12.08
24	0.8725	278.15	25.69	12.08
25	0.8725	278.15	-35.23	-16.47
26	0.8725	308.15	0.692	12.13
27	5.629	311.15	1.19	28.16
28	5.629	338.03	11.78	256.5
29	5.629	353.15	18.7	181.8
30	5.629	326.27	4.9	47.62
31	0.8725	326.27	4.9	47.62
32	101	300.15	0.669	0
33	101	305.15	8.102	1988
34	101	300.15	0.822	0
35	101	305.15	9.96	1090
36	101	285.15	27.54	0
37	101	280.15	53.48	1323
38	101	298.15	0	0
39	101	333.15	24.73	1283

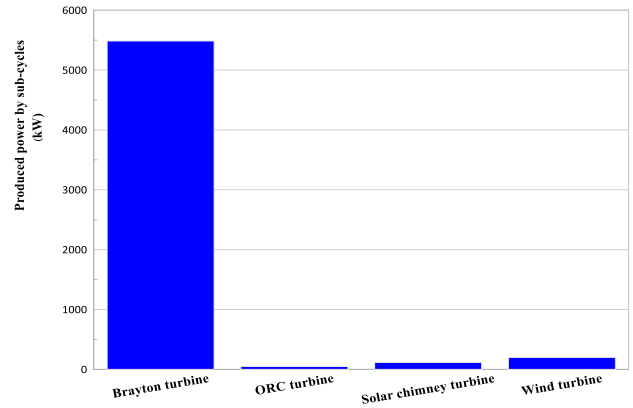


Figure 2. Production capacity by the proposed cycle subsystems

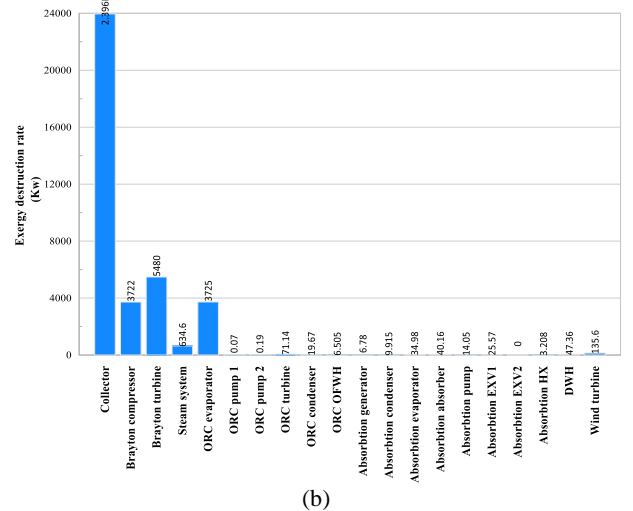
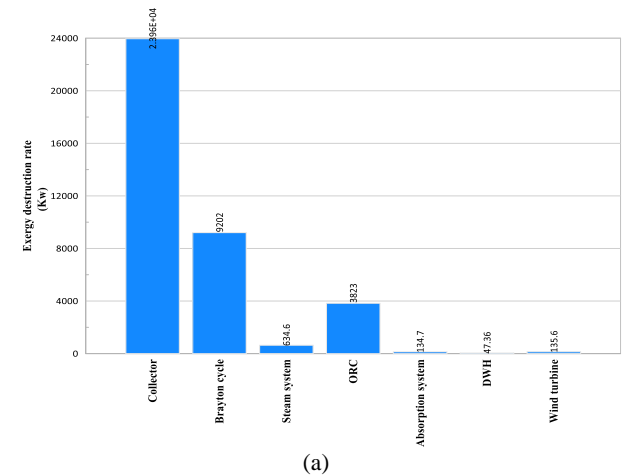


Figure 3. Exergy destruction rate (a) the main cycles (b) all system components

increases the amount of heat load and exergy to the system, which reduces the energy and exergy efficiency of the system.

Figure 5 shows the capital cost rate of the three proposed systems. The diagrams show that the highest cost rate belongs to system 3, in which a wind turbine and solar chimney are added to the first system. Brayton cycle turbines, the wind turbine, and solar chimney with values of 82515, 67759, and 33815 dollars per year have the highest capital cost rates, respectively, and special attention should be paid to these three components in the design of the system.

Figure 6 shows the relationship between the amount of solar radiation, the overall efficiency of the system, and

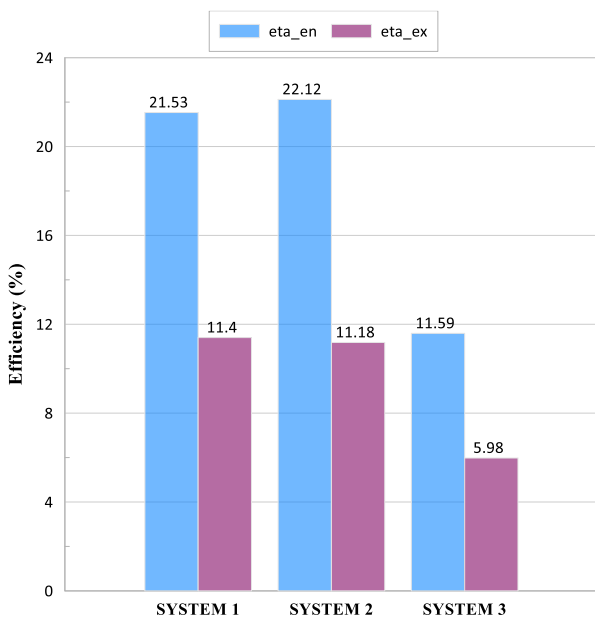


Figure 4. Energy and exergy efficiency of the proposed systems

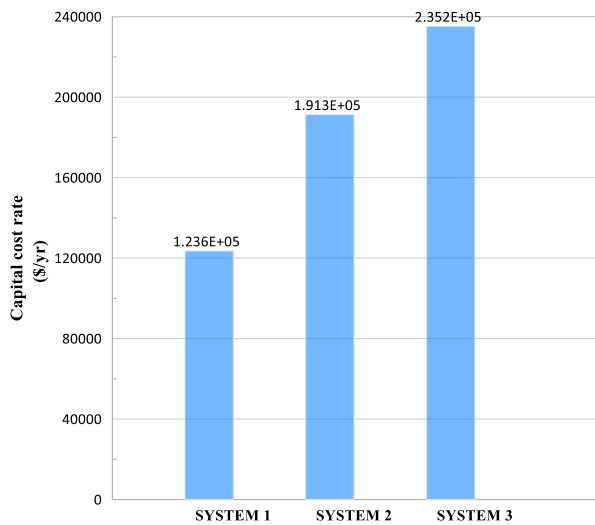


Figure 5. Capital cost rate of the proposed systems

the total cost of exergy destruction of the system. Investigation of the graphs proved that when the amount of solar radiation changes from 740 to 1040 W, the overall energy efficiency of the system decreases from 11.63 to 11.52% because the increase in solar radiation means that the amount of solar heat has a greater effect on the system. Therefore, the net effect on the overall energy efficiency is a decreasing trend. In addition, with the increase of solar radiation due to the addition of useful exergy, the exergy efficiency of the multigeneration system increases to about 0.43% and reaches 11.68% from 11.63%. Also, slightly increasing the amount of solar radiation significantly reduces the total cost of exergy destruction. This reduction is due to the availability of more useful work in more solar radiation, which reduces the amount of exergy destruction of the system components. Therefore, the total cost of destruction will be declining.

Figure 7 shows the energy and exergy efficiency of the general system by changing the inlet pressure of the Brayton cycle turbine. As a result of increasing the turbine inlet pressure from 750 kPa to 1500 kPa, the energy efficiency increases from 20.82% to 21.7 %, and the exergy efficiency rises from 9.63% to 10.58%. Based on the results, it can be stated that an increase in the turbine inlet pressure in the Brayton cycle has a positive effect on the system efficiency.

The effect of evaporator temperature on the energy and exergy efficiency coefficient of the absorption refrigeration system is displayed in Figure 8. Both operating parameters behave differently from the evaporator temperature. The energy efficiency coefficient increases from 0.62 to 0.7807 with increasing evaporator temperature from 273 K to 280 K, while the exergy efficiency decreases with an increase in evaporator temperature from 0.2386% to 0.2932%.

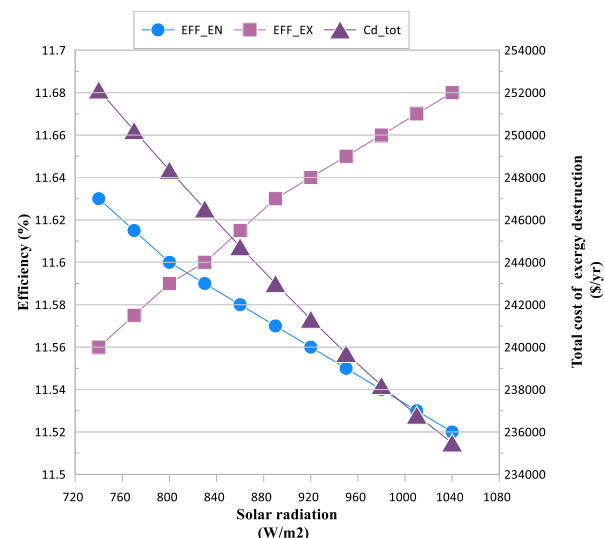


Figure 6. The effect of the amount of solar radiation on energy efficiency, exergy, and the total cost of system exergy destruction

The effect of wind speed changes on the wind turbine production capacity and system efficiency in terms of energy and exergy is depicted in Figure 9. The study of the diagrams shows that with increasing the inlet speed of the turbine, the wind turbine production capacity and the energy and exergy efficiency of the system increase. When the turbine speed increases from 4 to 12 m/s, the power generated by the turbine increases from 75.98 to 2051 kW. Also, the energy and exergy efficiency of the system increased from 11.18% to 18.69% and 11.37% to 14.72 %, respectively. The main reason for the increase in system efficiency is an increase in wind turbine

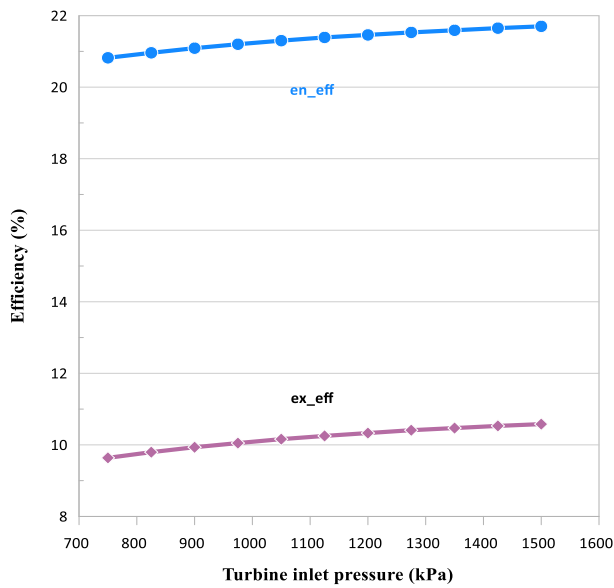


Figure 7. Energy and exergy efficiency of the overall system by changing the Brayton cycle turbine inlet pressure

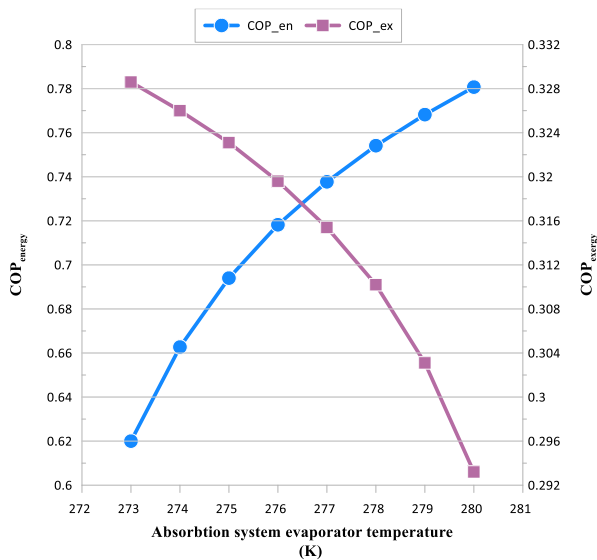


Figure 8. The effect of evaporator temperature changes on the energy and exergy COP of the absorption refrigeration system

production capacity by increasing the inlet speed of the turbine.

The net output of the system and the total cost of exergy destruction due to changes in the inlet temperature of the Organic Rankine cycle turbine are shown in Figure 10. According to the obtained graphs, by changing the temperature of the turbine from 373 to 433 K, the net output of the system first increases and then decreases. The optimum temperature for net output power is 400 K. Also, an increase in turbine inlet temperature, the total cost of system exergy destruction slightly decreases from \$241088 to \$240410 per year.

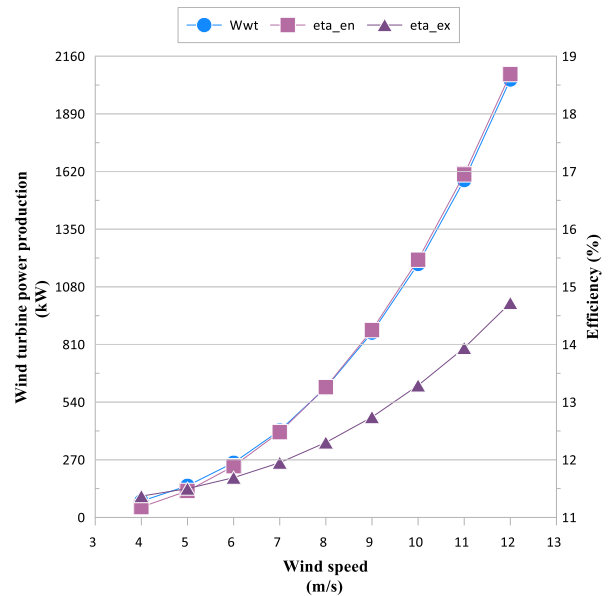


Figure 9. Impact of wind speed changes on wind turbine output capacity and system efficiency

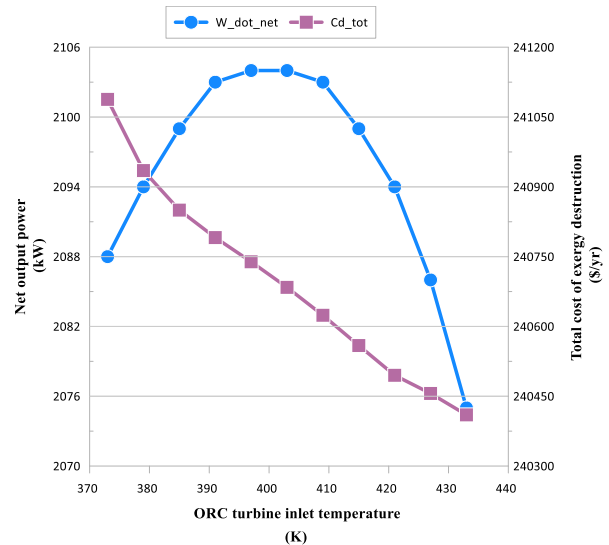


Figure 10. The effect of changing the ORC turbine inlet temperature on the net output power and the total cost of exergy destruction

CONCLUSION

In the present study, a multigeneration system is designed that uses a parabolic plate solar collector, wind turbine, and solar chimney to generate electricity, heating, cooling, hot water, and steam. Thermodynamic analysis of the system was performed using energy and exergy methods. The energy and exergy efficiency and the rate of exergy destruction of each component and the overall system were examined. In addition, a parametric study was performed to determine the effect of different parameters on the performance of the proposed system. Some of the outstanding results of this study can be expressed as follows.

- The highest energy and exergy efficiency of the multigeneration system was 22.12% and 11.4%, respectively.
- The total power generation capacity of the multigeneration system was calculated to be 2103 kW.
- The highest rate of exergy destruction for the main components of the system is seen in the solar collector. The Brayton turbine, compressor, and Organic Rankine cycle evaporator are other components with high exergy destruction. Therefore, to achieve better system efficiency, this amount of exergy destruction must be minimized.
- With increasing solar radiation, energy efficiency and the total cost of exergy destruction decreases, but the system exergy efficiency increases.
- The Brayton cycle turbine inlet pressure increase leads to the rise in the system efficiency.
- Increasing the evaporator temperature of the absorption refrigeration cycle increases the energy performance coefficient and decreases the exergy performance coefficient of the system.
- The higher the average wind turbine speed, the higher the efficiency and power generation.
- Increasing the inlet temperature of the Organic Rankine cycle turbine creates an optimal state for the net power produced by the system.

REFERENCES

1. Kazemian, M. E., Gandjalikhan Nassab, S. A. and Jahanshahi Javarana, E., 2021. Techno-economic Optimization of Combined Cooling, Heat and Power System Based on Response Surface Methodology, *Iranian (Iranica) Journal of Energy & Environment*, 12(4), pp. 285-296. Doi:10.5829/ijee.2021.12.04.02
2. Norouzi, N., 2021. Assessment of Technological Path of Hydrogen Energy Industry Development: A Review, *Iranian (Iranica) Journal of Energy & Environment*, 12(4), pp. 273-284. Doi:10.5829/ijee.2021.12.04.01
3. Bellos, E., Korres, D., Tzivanidis, C. and Antonopoulos, K., 2016. Design, simulation and optimization of a compound parabolic collector, *Sustainable Energy Technologies and Assessments*, 16, pp. 53-63. Doi:10.1016/j.seta.2016.04.005
4. Loni, R., Kasaeian, A., Mahian, O. and Sahin, A., 2016. Thermodynamic analysis of an organic rankine cycle using a tubular solar cavity receiver, *Energy conversion and management*, 127, pp. 494-503. Doi:10.1016/j.enconman.2016.09.007
5. Hafez, A., Soliman, A., El-Metwally, K. and Ismail, I., 2016. Solar parabolic dish Stirling engine system design, simulation, and thermal analysis, *Energy conversion and management*, 126, pp. 60-75. Doi:10.1016/j.enconman.2016.07.067
6. Abid, M., Ratlamwala, T. and Atikol, U., 2016. Performance assessment of parabolic dish and parabolic trough solar thermal power plant using nanofluids and molten salts, *International Journal of Energy Research*, 40(4), pp. 550-563. Doi:10.1002/er.3479
7. Cengel, Y. A., Boles, M. A. and Kanoğlu, M., 2011. Thermodynamics: an engineering approach. McGraw-hill New York.
8. Haaf, W., Friedrich, K., Mayr, G. and Schlaich, J., 1983. Solar chimneys part I: principle and construction of the pilot plant in Manzanares, *International Journal of solar energy*, 2(1), pp. 3-20. Doi:10.1080/01425918308909911
9. Zandian, A. and Ashjaee, M., 2013. The thermal efficiency improvement of a steam Rankine cycle by innovative design of a hybrid cooling tower and a solar chimney concept, *Renewable energy*, 51, pp. 465-473. Doi:10.1016/j.renene.2012.09.051
10. Esfandi, S., Baloochzadeh, S., Asayesh, M., Ehyaei, M. A., Ahmadi, A., Rabanian, A. A., Das, B., Costa, V. A. and Davarpanah, A., 2020. Energy, exergy, economic, and exergoenvironmental analyses of a novel hybrid system to produce electricity, cooling, and syngas, *Energies*, 13(23), pp. 6453. Doi:10.3390/en13236453
11. Méndez, C. and Bicer, Y., 2021. Integrated system based on solar chimney and wind energy for hybrid desalination via reverse osmosis and multi-stage flash with brine recovery, *Sustainable Energy Technologies and Assessments*, 44, pp. 101080. Doi:10.1016/J.SETA.2021.101080
12. Khan, M. S., Abid, M., Bashir, M. A., Amber, K. P., Khanmohammadi, S. and Yan, M., 2021. Thermodynamic and exergoeconomic analysis of a novel solar-assisted multigenerational system utilizing high temperature phase change material and hybrid nanofluid, *Energy Conversion and Management*, 236, pp. 113948. Doi:10.1016/J.ENCONMAN.2021.113948
13. Ngo, L. C., Bello-Ochende, T. and Meyer, J. 'Exergetic analysis and optimisation of a parabolic dish collector for low power application'. Proceedings of the postgraduate symposium, pp 22-23,
14. Yari, M., 2010. Exergetic analysis of various types of geothermal power plants, *Renewable energy*, 35(1), pp. 112-121. Doi:10.1016/J.RENENE.2009.07.023
15. Akrami, E., Khazaei, I. and Gholami, A., 2018. Comprehensive analysis of a multi-generation energy system by using an energy-exergy methodology for hot water, cooling, power and hydrogen production, *Applied Thermal Engineering*, 129, pp. 995-1001. Doi:10.1016/j.applthermaleng.2017.10.095
16. Ozlu, S. and Dincer, I., 2015. Development and analysis of a solar and wind energy based multigeneration system, *Solar Energy*, 122, pp. 1279-1295. Doi:10.1016/j.solener.2015.10.035
17. Klein, S. (2015). Engineering Equation Solver (EES) V9, F-chart software, Madison, USA.
18. Kalogirou, S. A., 2013. Solar energy engineering: processes and systems. Academic press. ISBN:0123972566
19. Assareh, E., Assareh, M., Alirahmi, S. M., Jalilinasrabad, S., Dejdari, A. and Izadi, M., 2021. An extensive thermo-economic evaluation and optimization of an integrated system empowered

- by solar-wind-ocean energy converter for electricity generation— Case study: Bandar Abas, Iran, *Thermal Science and Engineering Progress*, 25, pp. 100965. Doi:10.1016/j.tsep.2021.100965
20. Habibollahzade, A., Houshfar, E., Ahmadi, P., Behzadi, A. and Gholamian, E., 2018. Exergoeconomic assessment and multi-objective optimization of a solar chimney integrated with waste-to-energy, *Solar Energy*, 176, pp. 30-41. Doi:10.1016/j.solener.2018.10.016
21. Musharavati, F., Khanmohammadi, S., Pakseresht, A. and Khanmohammadi, S., 2021. Waste heat recovery in an intercooled gas turbine system: Exergo-economic analysis, triple objective optimization, and optimum state selection, *Journal of Cleaner Production*, 279, pp. 123428. Doi:10.1016/j.jclepro.2020.123428

COPYRIGHTS

©2021 The author(s). This is an open access article distributed under the terms of the Creative Commons Attribution (CC BY 4.0), which permits unrestricted use, distribution, and reproduction in any medium, as long as the original authors and source are cited. No permission is required from the authors or the publishers.



Persian Abstract

چکیده

هدف اصلی این مطالعه ارزیابی عملکرد ترمودینامیکی و اقتصادی استفاده از دودکش خورشیدی و توربین بادی جهت کمک به تولید برق در یک سیستم تولید چندگانه می باشد. سیستم پیشنهادی برای تولید توان، گرمایش، سرمایش، آب گرم و بخار به عنوان یک هدف چندگانه طراحی شده است. مطالعات پارامتری نیز برای بررسی اثرات پارامترهای مختلف مانند فشار ورودی توربین چرخه برایتون، دمای ورودی توربین چرخه رانکین آلی، تابش خورشیدی، سرعت باد و دمای اواپراتور چرخه تبرید جذبی بر کارایی سیستم مورد ارزیابی قرار می گیرد. تأثیر این پارامترها بر کارایی انرژی، انرژی و اقتصادی کل سیستم مورد بررسی قرار گرفت. نتایج نشان می دهد که بیشترین بازده انرژی و انرژی کلی سیستم تولید چندگانه به ترتیب ۲۲/۱۲ و ۱۱/۴ درصد به دست می آید. همچنین مجموع ظرفیت برق تولیدی سیستم مورد مطالعه ۲۱۰۳ کیلووات محاسبه گردید. نتایج نشان دادند که بیشترین میزان تخریب انرژی برای اجزای اصلی سیستم در کلکتور خورشیدی بشقابی دیده می شود. افزایش فشار ورودی توربین، سرعت متوسط باد ورودی توربین بادی و افزایش دمای اواپراتور چرخه تبرید جذبی تأثیر مثبتی بر روند کارایی سیستم پیشنهادی دارند.